Smart control of the multirotor drone propeller for enhanced vibration energy harvesting

SHPANIN, Leonid <http://orcid.org/0000-0002-3085-4678>, ABRAMIUK, Misko, GOODWIN, Matthew, PARAMESWARAN VEETTIL, Kannan Bernard, KARUVA CHALIL, Aasish, OSUCHUKWU, Nneka and PICKETT, Nicholas

Smart Control of the Multirotor Drone Propeller for Enhanced Vibration Energy Harvesting

Leonid Shpanin
Department of Engineering and Mathematics
Sheffield Hallam University
Sheffield, S1 1WB, UK
L.Shpanin@shu.ac.uk

Misko Abramiuk
Department of Engineering and Mathematics
Sheffield Hallam University
Sheffield, S1 1WB, UK
m.m.abramiuk@shu.ac.uk

Matthew Goodwin
Department of Engineering and Mathematics
Sheffield Hallam University
Sheffield, S1 1WB, UK
m.goodwin@shu.ac.uk

Kannan Bernard Parameswaran V.
School of Business and Management
University of Sunderland,
Sunderland, SR6 0DD, UK
kannan.bpv@gmail.com

Aasish Karuva Chalil
Department of Robotics and AI
Eternal Robotics PVT Ltd.,
Telangana, 500084, India
aasishkc@gmail.com

Nneka Osuchukwu
Department of Digital Asset
Egis Transport Solutions,
London, SE1 8QH, UK
nneka.osuchukwu@egis-group.com

Nicholas Pickett
Department of Engineering and Mathematics
Sheffield Hallam University,
Sheffield, S1 1WB, UK
n.j.pickett@shu.ac.uk

***Abstract*—This paper describes the technique of converting the multirotor drone propeller kinetic energy into electrical energy using piezoelectric industrial made components. The simulation and practical investigations of the novel energy harvester propeller structure and its control (with two industrially made piezoelectric elements which are located inside a single industrial made propeller) has been examined at different propeller rotational speeds. A novel propeller control technique for increasing electric energy production is being investigated using the smart drone motor control for enhanced propeller vibration and its energy harvesting performance. The proposed technique of the energy production for the multirotor drone operation is based on the drone propeller vibrations and aims to demonstrate that each propeller can harvest its own kinetic energy and convert it into the electrical energy which can be stored or used for different applications while the propellers are rotating. An attempt to model the energy production mechanism using SolidWorks and Creo pro engineer software is also made, examining the multirotor drone propellers at different operational conditions. All propeller simulations and practical tests were conducted under indoor laboratory conditions with suitable instrumentation. Analysis of the propeller vibration performance is presented via graphical representation of simulated and experimental results, to demonstrate that it is practically possible to recover the harvested energy from the vibrated propeller while the propeller is rotating. Consideration is given to using industrially made piezoelectric components for increasing the energy production mechanism in such concept. Photographic evidence of the test unit and setup of the propeller operation modes are presented and discussed together with experimental results to validate the theoretical concept via practical experimentation.**

1. Introduction

The multirotor drones provide a lot of opportunities for different applications, such as aerial mapping, heavy lifting for payload delivery, environment monitoring sensors and emergency purposes. From the previous authors works, different energy harvesting techniques have already been investigated practically for the multirotor drones' operation, where the energy recovery was produced from the Photovoltaic Cells (solar) [1], Thermoelectric Generators (heat) [2]. To harvest energy on board of the multirotor drone using its propellers is a very challenging task which provides an opportunity of using the self-sustained energy harvesting mechanism for propeller safety monitoring, wireless sensing for environment or propeller illumination in the dark environment. Recently, a new theoretical approach of extracting kinetic energy from the Gemfan 1147 ABS propeller of the multirotor drone was introduced theoretically by Osuchukwu *et al* [3]. The piezoelectric energy harvester for rotary motion applications was investigated previously [4, 5] demonstrating that using the piezoelectric materials is possible in the piezoelectric energy harvester structures.

In this contribution the authors validate the previously described concept [3] practically using the Tarot 1555 carbon propeller [6]. A piezoelectric material was used inside the propeller, converting the mechanical energy of the propeller into electrical energy. A novel technique of the energy production for the multirotor drone operation is based on the drone propeller vibrations aiming to demonstrate that each propeller can produce its own mechanical energy and transform it into electrical energy (while the propellers are rotating) which can be stored or used for various applications. A new propeller motor control technique is also being investigated for increasing the electric energy production by Tarot 1555 carbon propeller vibration which contains the encapsulated piezoelectric components. Analysis of the propeller vibration performance is discussed together with experimental results to validate the theoretical concept [3].

979-8-3503-0462-6/24/$31.00

2. Energy Harvester Unit Development

2A. Design Concept and CAD Modeling

The novel designed energy harvesting structure is based on the work which was reported by authors previously [3]. In this contribution, a large energy harvesting structure using the multirotor clockwise propeller of 1555 Tarot (which can harvest energy from the vibration of the propeller blade during its rotation) is developed. This is achieved by encapsulating two energy harvesting elements (PPA-1021 [7]) inside the propeller. The piezoelectric element is encapsulated inside the propeller to enhance the aerodynamics of the propeller since it doesn't affect the surface of the propeller. The conceptual design of the multirotor drone propeller in which two piezoelectric elements are encapsulated inside one propeller blade is shown in Figure 1. The position of the piezoelectric element inside the propeller determines the propeller vibration amplitude, vibration frequency and amount of energy harvested by propeller. Therefore, it was necessary to simulate one of the drone propellers and to find the optimal position of two piezoelectric elements located inside the

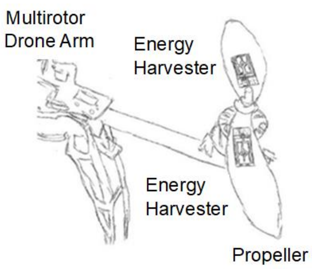

Figure 1. Conceptual design of piezoelectric energy harvesting system applied in a multirotor drone with 1555 Tarot propeller [4].

propeller. The ready-made CAD model of the 1555 Tarot propeller is not available in public domain. Therefore, to simulate the propeller operational conditions, the dimensions of the propeller were measured and incorporated into the propeller CAD model using SolidWorks [8] and Creo pro engineer [9] CAD software (Figure 2a, b). The developed propeller CAD model tolerance of +/- 5% is considered the largest error and is a reasonable representation of the real 1555 Tarot propeller [6].

(a) (b)

Figure 2. Clockwise Tarot 1555 carbon propeller shape identification: (a) Actual 1555 Tarot propeller [6], (b) SolidWorks CAD model propeller.

The diameter of the 1555 Tarot carbon propeller is chosen as 15 inches because encapsulating the piezoelectric element inside the propeller was easy to implement. The pitch of the propeller is 5.5 inch, and the weight of the propeller is measured as 20.2g. The piezo protection advantage (PPA) standard product of the rectangular piezoelectric package (designed for cantilever, bonded, and fixed beam configuration) was used in the energy harvester design. The PPA application ranges from vibration energy harvesting, vibration dampening, precise actuation, vibration, and strain sensing [7]. The PPA-1021 product (Figure 3a) was used as the most suitable structure to be encapsulated inside the 1555 Tarot propeller. The PPA-1021 was measured, and its CAD model was created on SolidWorks with +/- 2% error tolerance (Figure 3b). The CAD model was transferred to Creo Pro Engineer simulation package to evaluate the 1555 Tarot propeller deflection conditions. The parameters of the CAD model of the PZT-5H piezoelectric material was incorporated into SolidWorks as follows: density of 7700kg/m^3; Poisson ratio of 0.31; young's modulus of 6300Mpa; coefficient of thermal expansion of 1.17e^{-05}. The material property of the PZT-5H was assigned and two piezoelectric elements were encapsulated into the propeller blade at their optimal position.

Products	PPA-1011 PPA-2011 PPA-4011	PPA-1012	PPA-1013	PPA-1014 PPA-2014	PPA-1021
Length (mm) [mils]	(71.0) [2.80]	(71.0) [2.80]	(71.0) [2.80]	(53.0) [2.09]	(71.0) [2.80]
Width (mm) [mils]	(25.4) [1.00]	(41.5) [1.63]	(41.5) [1.63]	(20.8) [0.82]	(10.3) [0.41]
Thickness (mm) [mils]	(0.71) [28.0] (0.76) [30.0] (1.32) [52.0]	(0.75) [29.5] (0.80) [31.5]	(1.94) [76.5]	(0.74) [29.0] (0.83) [32.5]	(0.74) [29.0] (0.86) [34.0]
Piezo Length (mm) [mils]	(46.0) [1.81]	(46.0) [1.81]	(46.0) [1.81]	(27.8) [1.09]	(46.0) [1.81]
Piezo Width (mm) [mils]	(20.8) [0.82]	(38.4) [1.51]	(33.4) [1.31]	(18.0) [0.71]	(06.4) [0.25]
Piezo Thickness (mm) [mils]	(0.18) [06.0]	(0.25) [10.0]	(1.47) [58.0]	(0.19) [07.5]	(0.25) [10.0]
Number of Piezo Layers	1 2 4	1	1	1 2	1
Piezo Materials	PZT-5H	PZT-5H	PZT-5H	PZT-5H	PZT-5H
Capacitance (nF)	97 190 415	120	24	41 94	22
Mass (grams)	3.0 4.0 7.6	6.0	21.5	2.0 2.9	1.4

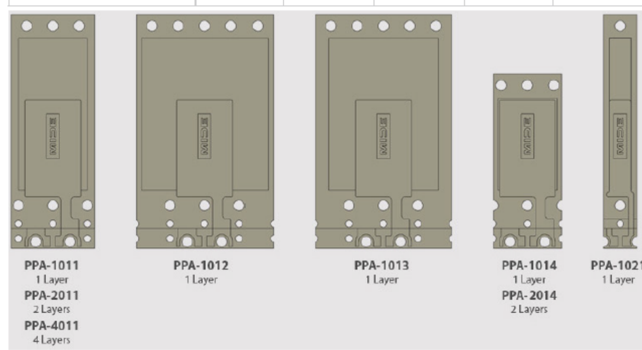

(a)

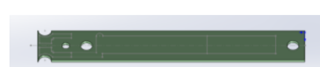

(b)

Figure 3. Piezoelectric element ranges [7]: (a) Parameters of the PPA products, (b) View of the PZT-5H piezoelectric element CAD model constructed.

2B Energy Harvester Computational Results

The designed CAD propeller model in SolidWorks was loaded into Creo pro engineer simulation software (without the piezoelectric element inside the propeller) and the static (constant) propeller rotation was simulated from 1000rpm to 10,000rpm (revolution per minute) to find the maximum deflection point on the propeller, and to decide the optimal position for the encapsulation of the piezoelectric element (Table 1). The mesh properties of CAD propeller model in SOLIDWORKS used in simulations were as follows: Mesh type - Solid mesh; Mesher used - Curvature bases Mesh; Max. / Min. Element Size of 1.12591mm / 0.12565mm; Total Nodes of 165398; Total Elements of 103569.

Table 1. Creo pro engineer simulated propeller results without the piezoelectric element inside the propeller.

Test	SPEED (rpm)	Deflection (mm)
1	1081	0.0133
2	2006	0.045
3	3002	0.1027
4	4007	0.183
5	5016	0.286
6	6003	0.411
7	7007	0.55
8	7983	0.726
9	9000	0.923
10	10000	1.14

The parameters of the carbon fiber is pre-loaded to the Creo pro engineer software, as: Density of 1780kg/m^3; Poison ratio of 0.26; Young's modulus of 350Gpa and coefficient of thermal expansion of 5.944e^{-05}/c. After the material property was added, the mesh control was included, in which the entire CAD model was selected, and meshing was applied. Figure 4 demonstrates a typical example of the propeller deflection at 4007rpm where different colour indicates the amount of deflection in the propeller (i.e., the red portion indicates the maximum deflection point, and the dark blue indicates the zero-deflection point). The optimal position is the yellowish-green portion of the propeller since the piezoelectric element can be encapsulated inside the thick portion of the blade. Once the position of the piezoelectric elements was determined the CAD model of the piezoelectric elements was developed and included inside the propeller structure. The piezoelectric element was measured accurately, and the model was created with +/- 2% error tolerance. An example of a full CAD structure of the 1555 Tarot propeller with the encapsulated piezoelectric elements PPA-1021 is shown in Figure 5 and it was investigated using the Creo pro engineer simulation software. Simulation was carried out from 1000rpm to 10,000rpm to find the maximum deflection point on the propeller with the piezoelectric components included (Table 2, Figure 6). Figure 6 demonstrates the propeller deflection at 4007rpm with maximum deflection marked as red and the non-deflected zone as blue colours.

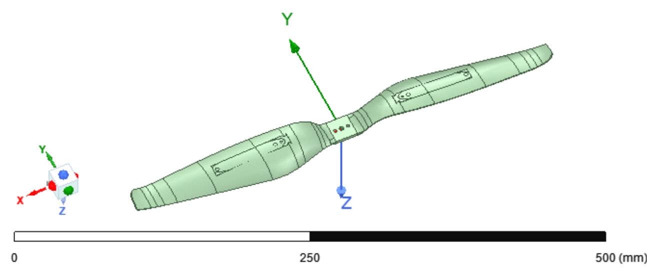

Figure 5. An example of the simulated CAD structure of the 1555 Tarot propeller with the encapsulated piezoelectric elements PPA-1021.

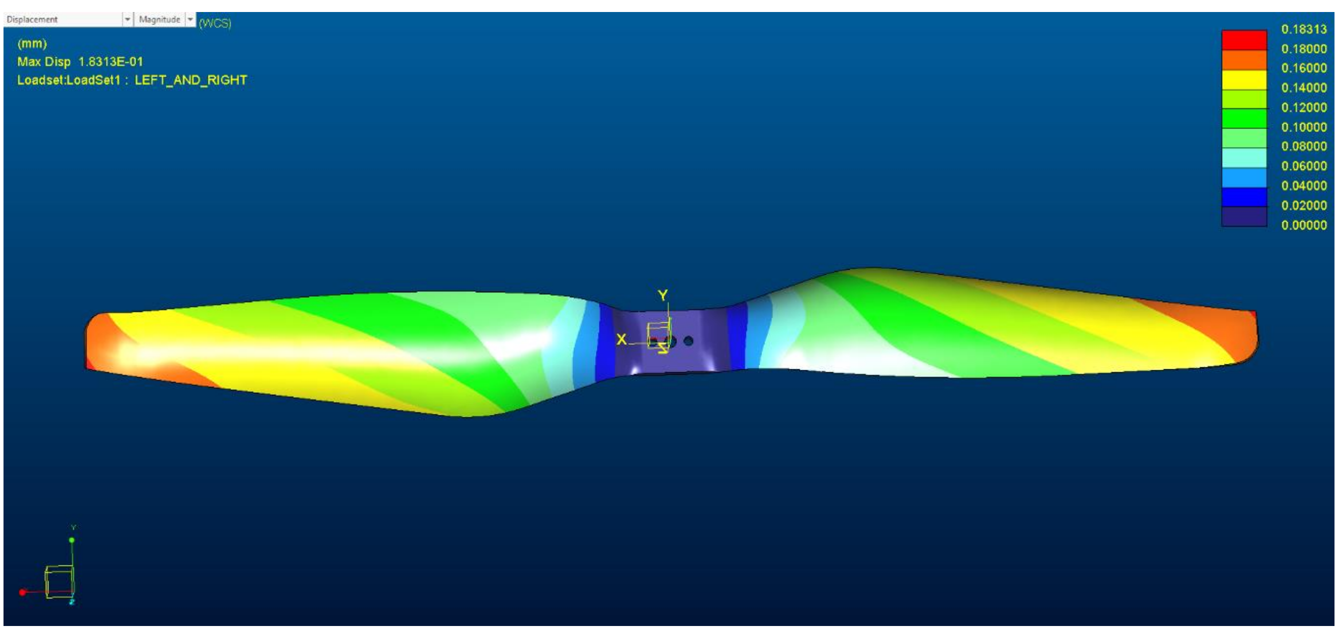

Figure 4. Deflection of the 1555 Tarot propeller at 4007rpm without the encapsulated piezoelectric element included.

Table 2. Creo pro engineer simulated propeller results with the piezoelectric element inside the propeller.

Test	SPEED (rpm)	Deflection (mm)
1	1081	0.0245
2	2006	0.083
3	3002	0.187
4	4007	0.337
5	5016	0.524
6	6003	0.757
7	7007	1.023
8	7983	1.339
9	9000	1.703
10	10000	2.084

Table 3. Theoretical result of the static propeller thrust without the piezoelectric element inside the propeller calculated by the online thrust calculator [10, 11].

Test	Speed (rpm)	Thrust (N)	Thrust (kg)
1	2113	2.65	0.27
2	2400	3.43	0.35
3	2830	4.81	0.49
4	3295	6.57	0.67
5	4018	9.81	1
6	4650	13.24	1.35
7	5580	19.03	1.94
8	6219	23.63	2.41

The propeller deflection at additional rpm values is shown in the section "Appendix". The simulation results shown on Table 2 indicate that the propeller deflection has increased almost twice in comparison with Table 1. Since the 1555 Tarot propeller simulation geometry is not ideal, the online thrust calculator [10, 11] was used to predict the 1555 Tarot propeller thrust theoretically (Table 3) and then to compare the simulation results with the experimental results (Table 4).

C. Energy Harvester Construction and Test

Manufacturing of the propeller energy harvester was implemented at the Sheffield Hallam University's workshop, and it is shown in Figure 7a, b. Two lead wires are soldered to the copper ends of each piezoelectric element (PPA-1021) and are connected to the equipment for monitoring the voltage harvested by each piezoelectric element. Two piezoelectric elements are glued inside the latches made by

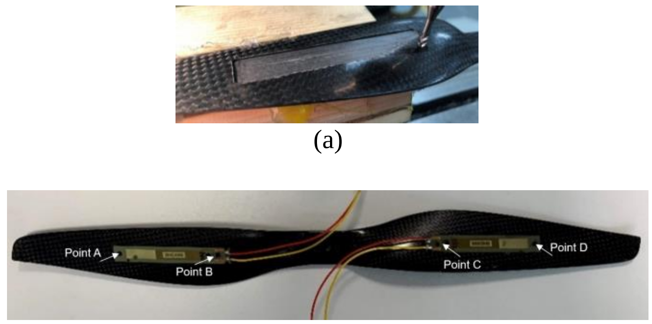

(a)

(b)

Figure 7. Energy harvester unit construction: (a) Milling process on the 1555 Tarot propeller blade [6] to remove material for the piezoelectric element, (b) View of two piezoelectric elements (PPA-1021, [7]) glued on surface of the 1555 Tarot propeller [6] in points A, B, C and D.

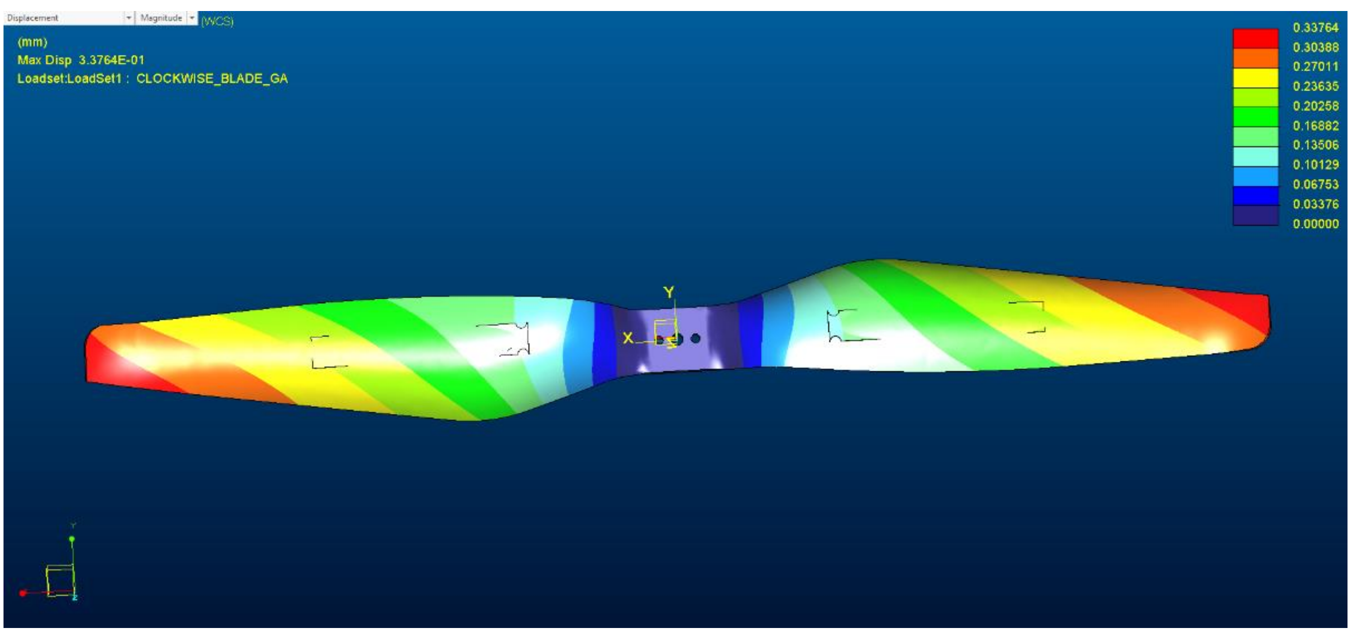

Figure 6. Deflection of the 1555 Tarot propeller at 4007rpm with encapsulated piezoelectric elements included.

milling. Only at the tips of the PPA-1021, the piezo elements are glued so that each piezoelectric element is not restricted from its natural vibration during the motion (the piezoelectric element is only present at the center of the device which is protected by using the epoxy resin). The PPA-1021 piezoelectric element was glued on to the milled gap of the 1555 Tarot propeller which ensures the aerodynamics of the propeller. Initially, to validate the CAD model, the 1555 Tarot propeller (without the piezoelectric elements locating inside the propeller) was tested practically. The propeller was mounted on top of the Hengli KV 370 brushless motor [12], the motor was successfully screwed on top of the test rig and the entire rig was kept on top of the weighing machine and the machine reading was made to zero to eliminate the weight of the motor-test rig setup. Gradually the motor rpm was controlled by using a remote control and the static propeller thrust in kg was measured from the weighing machine reading. Since the clockwise blade was used for testing, the motor direction was chosen accordingly. Once the reading from low rpm to highest possible was taken and the propeller thrust was noted in kg it was converted to Newton (N) (where: 1kg = 9.8 N) [10, 11]. The obtained practical results of the propeller thrust (shown on Table 4 for different propellers' rpm) are 20% - 30% lower than online theoretical thrust calculator data shown on Table 3, [11] indicating that they are in fair to good agreement with the theory.

Table 4. The practical results of the 1555 Tarot propeller static thrust without the PPA-1021 component.

Test	Speed (rpm)	Thrust (N)	Thrust (kg)
1	2113	1.78	0.182
2	2400	2.15	0.22
3	2830	3.04	0.31
4	3295	3.92	0.4
5	4018	6.76	0.69
6	4650	10.78	1.1
7	5580	16.69	1.7
8	6219	18.63	1.9

The practical results indicate that the produced CAD model of the 1555 Tarot propeller geometry is not ideal. In addition, the practical test conditions were not ideal due to the friction in the air or error in the indicated value on the weighing device. Thus, further improvement of the 1555 Tarot CAD propeller geometry and propeller practical tests without the PPA-1021 piezoelectric element included will be needed to narrow the gap between the theoretical and simulated results. In addition, the static thrust measurements were necessary to ensure the proper range of 1555 Tarot propeller and Hengli KV 370 brushless motor operation prior to testing the motor and propeller at different motor control modes. The practical earth-stationary propeller thrust measurements were important as the multirotor drone could operate at low speeds relative to earth.

3. Control Techniques of the Test Unit

The primary aim of this contribution is to find an optimal operational condition of the energy harvester unit, described in Section 2, where a maximum energy harvester voltage can be produced by PPA-1021 element encapsulated inside the 1555 Tarot propeller. Therefore, two motor control modes were investigated, where Hengli KV 370 brushless motor [12] (connected with the 1555 Tarot propeller) was connected in series with the DJI electronic speed controller (ESC) Takyon Z318 (18A / 2-3S LiPo using OneShot125 PMW protocol, with 125µs (stop) and 250µs (full power), [13, 14] and the Keysight 33500B Series Trueform Waveform Generator which produced the different signal for the motor operation. In the first motor control mode, a constant PWM signal produced by the Waveform Generator was used to control the motor speed. In the second motor control mode, the pulse width (PW) controlling motor speed is modulated at frequency matching the free (natural) vibrational frequency of the propeller. The modulation signal depth was a nominal of 20µs which controls the change of the propeller speed. This was introduced to evaluate the propeller rotational impact on the produced voltage of the single piezoelectric energy harvester with a minimum propeller thrust change. Figure 8 introduces the test layout of the equipment which was used to conduct the tests. The piezo element lead wires were connected through the robust (pre-built) slip ring contacts' structure (to measure the signal in the time domain) using the Rohde & Schwarz RTE 1024 oscilloscope (Figure 8) and Pico Scope 5203 (to measure the signal in the frequency domain, Figure 8). The rotational speed of the propeller was monitored through the hole slotted optical switch (sensor) shown in Figure 8.

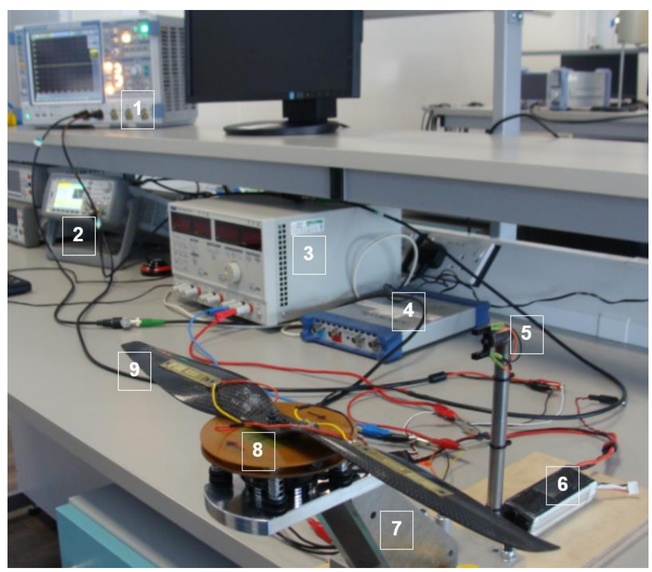

Figure 8. Layout of the propeller test unit (where: 1 - Oscilloscope; 2 - Waveform Generator; 3 - Power supply for the propeller speed sensor; 4 - PicoScope; 5 - Propeller speed sensor; 6 - LiPo battery; 7 – Metal support structure; 8 - Slip ring contacts' structure; 9 - propeller with two glued piezoelectric elements.

4. Experimental Results And Discussion

4A. Static Drone Motor Control Mode

From the datasheet of PPA-1021, the piezoelectric element is capable of harvesting energy in the range of 22Hz - 175Hz of its resonant vibration frequency, producing the RMS voltage output in the range of 1.2V - 28.2V, RMS current of up to 0.2mA and the RMS power of up to 4.5mW [7]. The above parameters depend on the PPA-1021 peak to peak propeller deflection [3] which varies between 0.6mm and 16.1mm [7]. It also depends on the tip mass which is usually mounted on top of the piezo element's end which helps to produce larger piezo element deflection [7]. However, from the previous theoretical investigation [3] (and current simulation results shown on Tables 1 and 2) the tip mass can be ignored to be used as the propeller deflection is produced once it starts to rotate. Considering the above piezo element paraments, a resonant frequency of the 1555 Tarot propeller (with the fixed PPA-1021 elements inside the propeller) mounted on top of the Hengli KV 370 brushless motor (Figure 9) was measured.

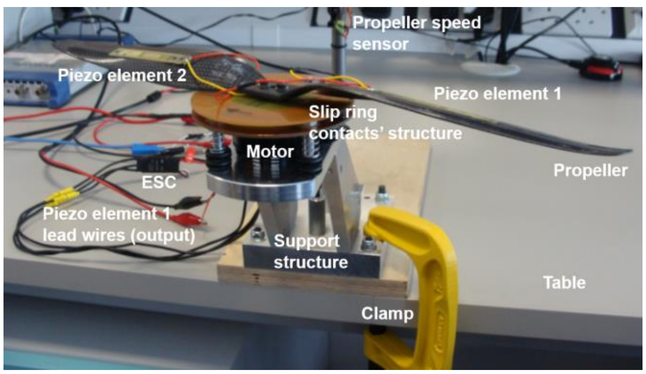

Figure 9. Setup of the test unit for the piezo elements 1 and 2 vibration frequency measurements.

To monitor the resonant frequency of the PPA-1021 component, one end of the propeller (close to the piezo element 1) was disturbed manually to monitor the propeller vibration frequency via two lead wires connected to the Rohde & Schwarz RTE 1024 oscilloscope (to measure in time domain) shown in Figure 10 and PicoScope 5203 (to measure in frequency domain) shown in Figure 11. A similar signal behavior was found in both piezoelectric elements locating inside the propeller) as the location of the piezoelectric elements are symmetrical in relation to the propeller structure (Figure 7b). The experimental tests under the static (constant) motor rotational speed (rpm), using the test setup shown in Figure 8, were conducted and results are tabulated on Table 5. The practical tests were taken between 2000 and 3000rpm of the propeller rotation (using the

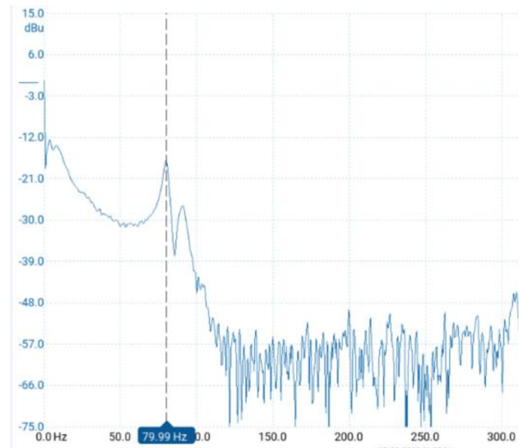

Figure 11. The propeller natural frequency vibration of 79.99Hz (without the motor rotation) in the frequency domain (where: the vertical axis is in dBu (voltage in logarithmic scale) and a horizontal axis is in Hertz).

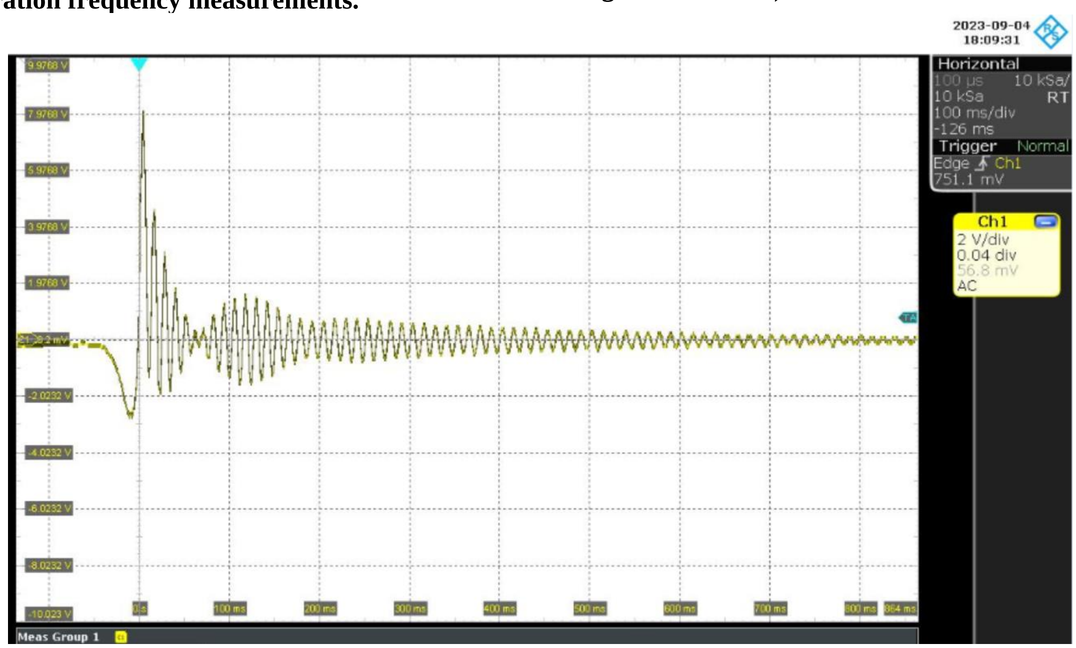

Figure 10. Output voltage of the piezoelectric element of natural frequency vibration (without the motor rotation) in the time domain (where: the vertical axis is in Volts and a horizontal axis is in milliseconds).

2200mAh 11.1V 3S 25C LiPo battery as a power supply connected to the ESC and motor in series) provided a real test condition of one arm multirotor drone operation. Two lead wires from the piezoelectric element (Figure 7b) were connected directly to the oscilloscope. The circuit was operated without the current load. The peak-to peak voltage of the piezoelectric element was monitored at different rpm to see how the produced piezoelectric voltage (without the load resistor used) behaves at different propeller rotational speeds. It was found that between 1974rpm and 2895rpm the piezoelectric component produced the noisy (close to sinusoidal shape) output voltage between 0.8V (100Hz vibration frequency) and 2.2V (62Hz) respectively.

Table 5. The practical results of the 1555 Tarot propeller, with the PPA-1021 piezoelectric element located inside the propeller without the modulated Hengli KV 370 motor rotation (without the load resistor used).

Test	Propeller rotational speed (rpm)	Piezoelectric vibration frequency (Hz)	Piezoelectric peak-to-peak output voltage (V)
1	1974	100	0.8
2	2352	75	1.6
3	2895	62	2.2

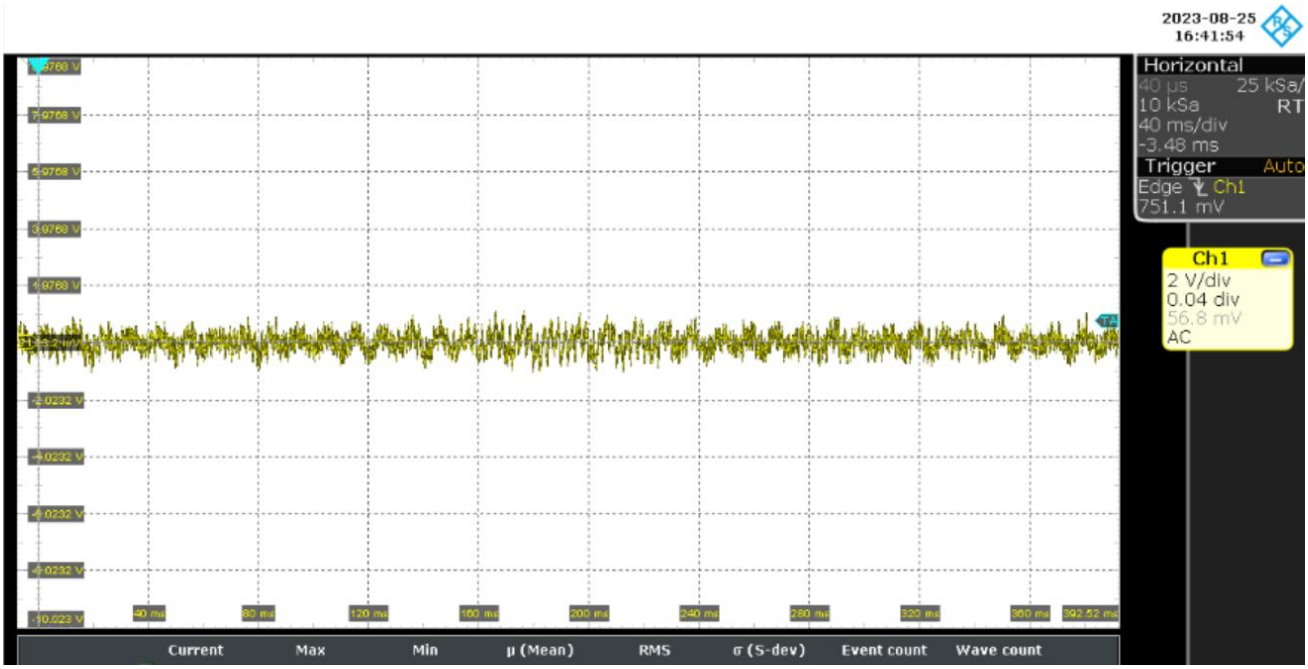

Figure 12. Piezo element produced voltage at static propeller rotation of 1974rpm without the motor modulation and without the piezoelectric load.

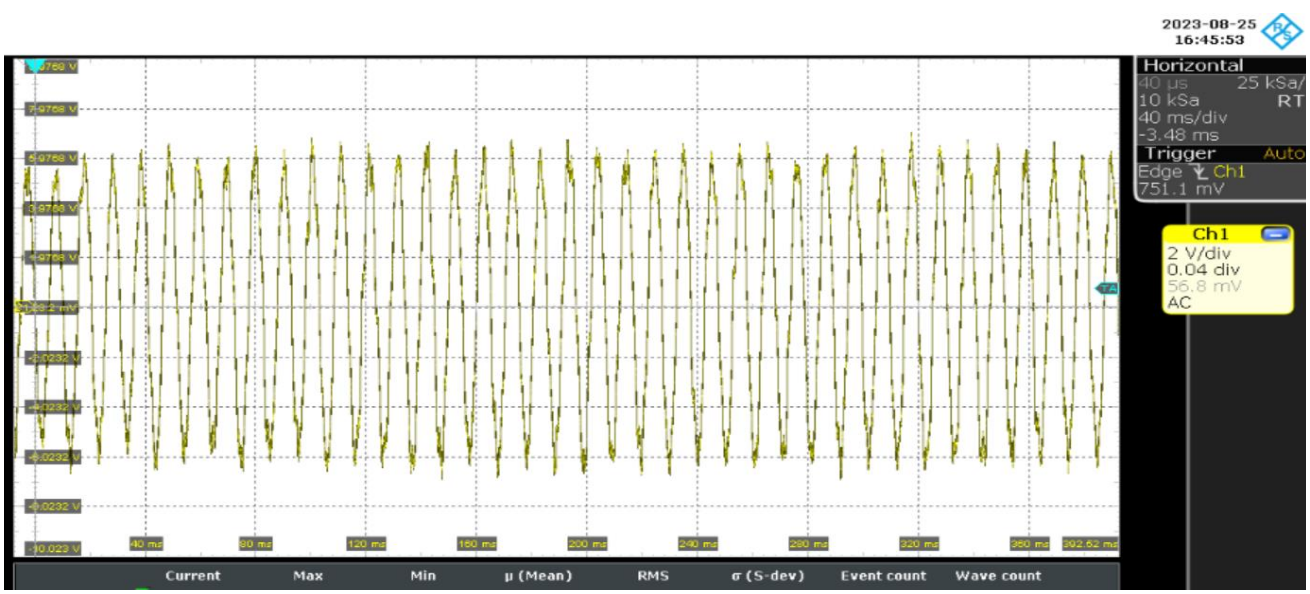

Figure 13. Piezo element produced voltage with the propeller modulated motor rotation of 1974rpm and without the piezoelectric load.

An example of the piezo element produced voltage is shown in Figure 12, where a vertical axis is in Volts and a horizontal axis is in seconds.

4B. Modulation Drone Motor Control Mode

The practical tests of the same test setup (shown in Figure 8) with the propeller rotation modulation were conducted. The obtained results are shown in Figure 13 and on Table 6.

Table 6. The practical results of the 1555 Tarot propeller, with the PPA-1021 piezoelectric element located inside the propeller with the modulated Hengli KV 370 motor rotation (without the load resistor used).

Test	Propeller rotational speed (rpm)	PW/Propeller modulation frequency (Hz)	Piezoelectric peak-to-peak output voltage (V)
1	1974	97	12
2	2352	103	10
3	2895	110	7

It was found that at the propeller rotation of 1974rpm the piezoelectric output produced a continues oscillated voltage of 12V peak-to-peak with the PW / propeller modulation frequency of 97Hz (Table 6). The piezoelectric output is reduced to 7V peak-to-peak at the higher propeller rotation of 2895rpm having the PW / propeller modulation frequency of 110Hz. Figure 13 demonstrates the energy harvested signal produced by a single PPA-1021 piezoelectric element (located inside the propeller, Figure 7b) at the constant propeller rotation of 1974rpm.

4C. Discussion

The experimental results of the energy harvester PPA-1021 element between 2000rpm and 3000rpm of the propeller rotation (without the load resistor connected between two output lead wires of the piezo element) suggested that the motor that forces the propeller to rotate should be controlled with a sinusoidal modulated signal close to the natural propeller vibration frequency of 80-90Hz as shown in Figures 10 and 11. In this condition one PPA-1021 element should produce a maximum voltage amplitude. To evaluate the piezoelectric harvested power of one piezoelectric element at the 1974rpm of the propeller rotation, the test setup shown in Figure 8 was used with 3-test settings (Tests 1, 2 and 3) without the motor modulation (Table 7) and with the motor modulation (Table 8). The load resistors of 81.8kΩ, 99.1kΩ and 118.8kΩ, connected separately between two lead wires of the piezoelectric element (Figure 7b) were used (in both test modes) to examine the piezo element produced RMS power once the propeller is rotated at constant (or modulated) rotational speed of 1974rpm. It was found that once the piezoelectric load resistance increases from 81.8kΩ to 118.8kΩ, the harvested peak voltage of the piezo element stays relatively the same in the range of 0.4V at constant propeller rotational speed (Table 7). The harvested power (in RMS) of one piezo element was calculated as 0.96μW (for 81.8kΩ load resistor) and 0.66μW (for 118.8kΩ load resistor). In this mode, the best test condition is Test 2 which produced the piezo element RMS power of 1.78μW.

Table 7. The practical results of the 1555 Tarot propeller, with the PPA-1021 piezoelectric element located inside the propeller & without the modulated Hengli KV 370 motor rotation (the tests are with the load resistor used at the propeller rotational speed of 1974rpm).

PPA-1021Test characteristics	Test 1	Test 2	Test 3
Piezoelectric load, (kΩ)	81.8	99.1	118.8
Peak voltage of the sinusoidal signal, (V)	0.4	0.6	0.4
RMS voltage of the sinusoidal signal, (V)	0.28	0.42	0.28
Produced power, in RMS, (μW)	0.96	1.78	0.66

The obtained results, shown on Table 8, indicate how the PPA-1021 piezoelectric output characteristics of one piezo element (i.e., the resonant vibration frequency and produced peak voltage) behave at 1974rpm of the propeller rotational speed once the motor mode modulation is introduced. In this mode, the OneShot125 PWM protocol pulse width of 184μs with 20μs of the signal modulation depth (produced by Waveform Generator) was used, which provides 16 changes of the pulse width time per one period of the produced piezoelectric vibration frequency. This was considered as an optimal condition in controlling the ESC Z318 operation. It was found that once the piezoelectric load resistance increases from 81.8kΩ to 118.8kΩ, the harvested peak voltage of the piezo element increased significantly from 3.5V to 5.5V. The propeller modulation frequency was in the range of 102Hz and 99Hz respectively.

Table 8. The practical results of the 1555 Tarot propeller, with the PPA-1021 piezoelectric element located inside the propeller & with the modulated Hengli KV 370 motor rotation (the tests are with the load resistor used at the propeller rotational speed of 1974rpm).

PPA-1021 Test characteristics	Test 1	Test 2	Test 3
Piezoelectric load, (kΩ)	81.8	99.1	118.8
PW/Propeller modulation frequency, (Hz)	102.0	97.0	99.0
Peak voltage of the sinusoidal signal, (V)	3.5	5.0	5.5
RMS voltage of the sinusoidal signal, (V)	2.5	3.5	3.9
Produced power, in RMS, (mW)	0.08	0.12	0.13

The harvested power (in RMS) of one piezo element was calculated as 0.08mW (for 81.8kΩ load resistor) and 0.13mW (for 118.8kΩ load resistor, which is considered as the best performance of this test mode). The RMS power generated by one piezo element of 0.13mW at 1974rpm of the propeller rotation is in a good agreement with the piezo element PPA-1021 datasheet [7] where the piezo element should be deflected (peak-to peak) less than 0.1mm (peak-to-peak) and produce the RMS power of up to 0.2mW. This trend was confirmed by the simulation results at 2006rpm of the propeller rotation (Table 2) where the propeller deflection was less than 0.1mm (peak) at 2006rpm.

In addition, from the obtained results tabulated on Table 8, it should be noticed that the propeller configuration shown in Figure 7b could produce at least 0.26mW where two piezo elements (connected in parallel) could combine the RMS power at the propeller rotational speed of 1974rpm. This power could be used to supply the sensor circuit located on the surface of the propeller which can monitor the propeller in the discrete time mode. Furthermore, from the Figure 3a (and PPA products' datasheet, [7]) it was indicated that the piezoelectric element PPA-1021 can be replaced to the larger power (single layer) piezoelectric energy harvester element of similar geometry, such as PPA-1011 or PPA-1014 [7]. This option could potentially harvest the piezo element RMS power up to 16.0mW and 25.9mW respectively. As a result, one propeller with two piezo elements locating inside one propeller could potentially produce a double combined harvested RMS power of 32mW and 51.8mW respectively. The range of the produced power could be sufficient to supply the wireless sensor circuit in the continuous time mode, which can be installed on the surface of the propeller for sensing purposes during the multirotor drone take-off and landing. Finally, the customaries shape of the piezo element (for example its length and width) located inside the propeller could significantly increase its harvested power as the larger piezo element peak-to-peak deflection the larger power could be produced.

5. CONCLUSIONS

The study of the multirotor drone propeller energy harvester has been investigated in this paper. The propeller simulation and practical study of the novel energy harvester propeller structure and its control with two industrially built piezoelectric elements (locating inside the industrially built propeller) has been examined at different propeller rotational speeds. It was concluded that using the above technique it is practically possible to harvest the RMS power of 0.13mW from a single piezoelectric element, which can then be stored. The produced power could be higher using the suitable piezoelectric elements, circuit arrangement and control. Further work is needed to optimize the energy harvester structure for the drone propeller sensor circuits, monitoring the propellers and drone safety during the drone take-off, flight, and landing modes.

APPENDIX

The Creo pro engineer simulation results of the 1555 Tarot propeller with two embedded PPA-1021 piezo elements (Figure 5) at 1081rpm and 6003rpm values are shown in Figures A1 and A2. The maximum propeller deflection is observed as 0.0245mm and 0.757mm respectively (Table 2).

ACKNOWLEDGEMENTS

The authors appreciate the support provided by Sheffield Hallam University, UK, that has funded this work as well as the senior technicians of computer aided engineering Mr. Steven Brandon and Mr. Steven Worsley for their assistance in the CAD modeling.

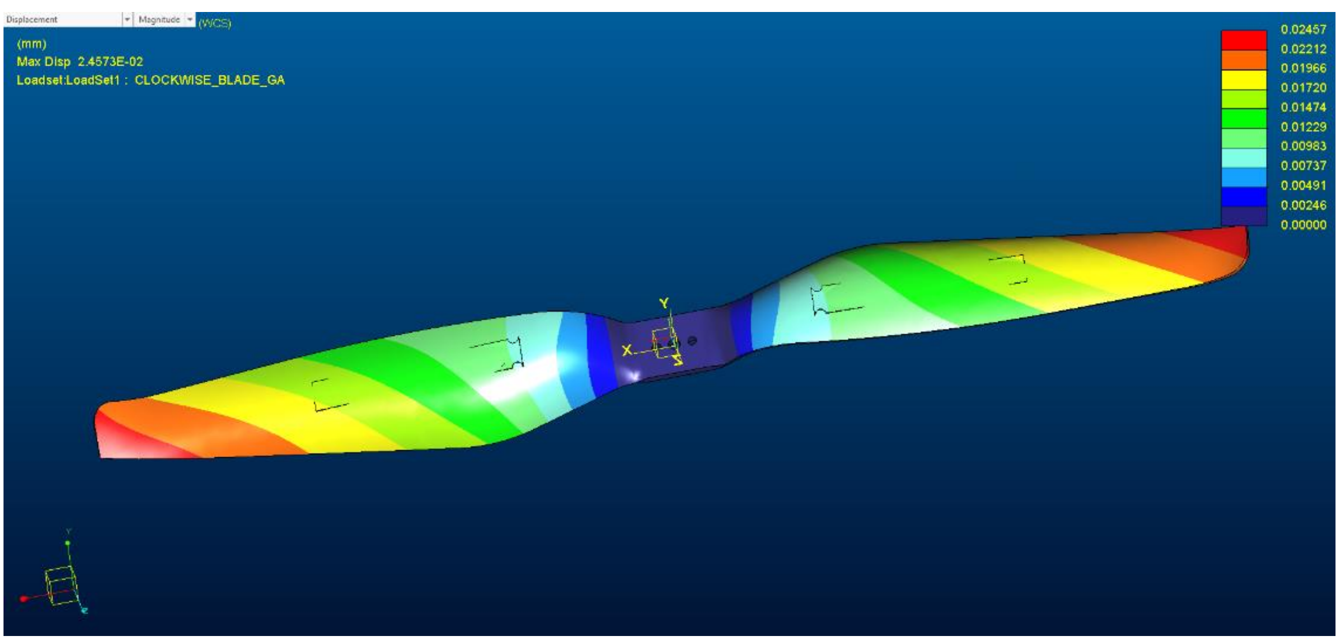

Figure A1. Deflection of the 1555 Tarot propeller at 1081rpm with encapsulated piezoelectric elements included.

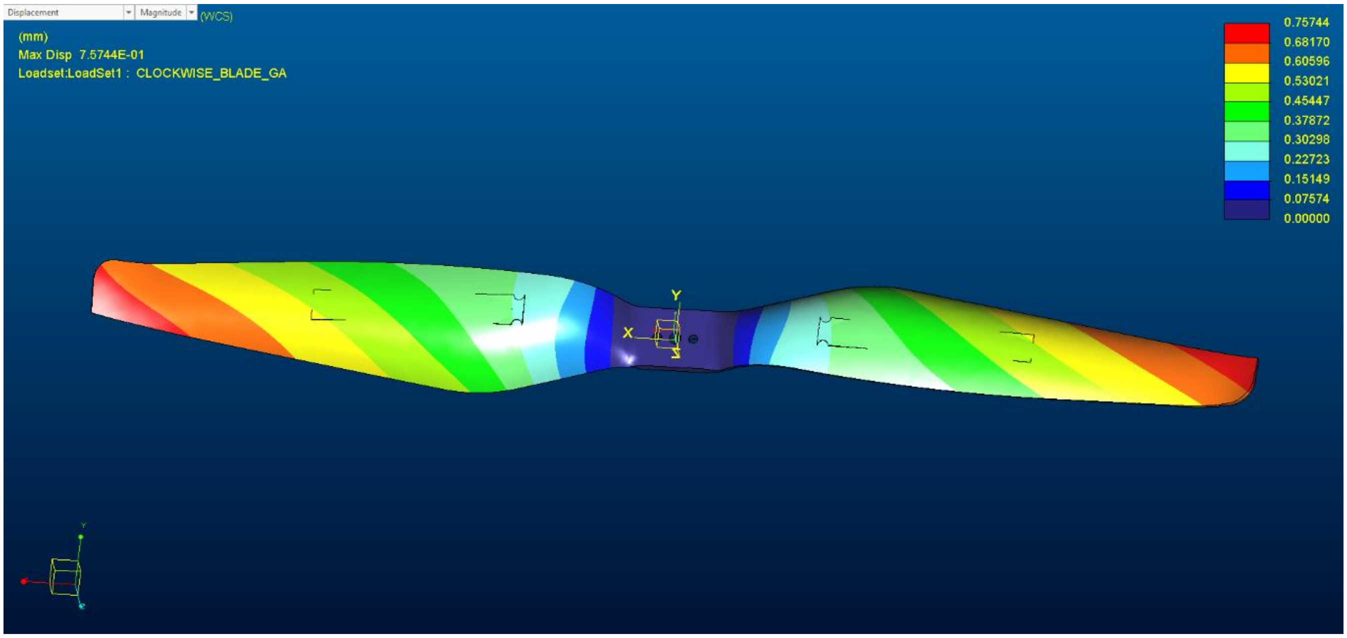

Figure A2. Deflection of the 1555 Tarot propeller at 6003rpm with encapsulated piezoelectric elements included.

References

[1] Shaheed M., Abidali A., Ahmed J., Ahmed S., Burba I., Fani P., Kwofie G., Wojewoda K. and Munjiza A., "Flying by the Sun only: The Solarcopter prototype", *Aerosp. Sci. and Techn.*, Vol. 45, pp.209-214, 2015.

[2] J. Fleming, W. Ng and S. Ghamaty, "Thermoelectric-Based Power System for Unmanned-Air-Vehicle/ Microair-Vehicle Applications", *J. of Aircraft*, 41(3), pp.674-676, 2004.

[3] Osuchukwu N. and Shpanin L., "Feasibility Study of the Quadcopter Propeller Vibrations for the Energy Production", *Int. J. of Mech., Aerosp., Industr., Mechatr. and Manufact. Eng.*, Vol. 11 No. 2: pp.277-283, Feb. 2017.

[4] F. Khameneifar, S. Arzanpour, and M. Moallem, "A piezoelectric energy harvester for rotary motion applications: Design and Experiments", *IEEE/ASME Trans. on Mechatr.*, vol. 18, (5), pp.1527-1534, 2013.

[5] A. Erturk and D. Inman, "On mechanical modeling of cantilevered piezoelectric vibration energy harvesters," *J. Intell. Mater. Syst. Struct.*, vol. 19, pp.1311-1325, 2008.

[6] 1555 Tarot propeller Web site: www.rchobby-avenues.co.uk/tarot-1555-carbon-propellers-two-holes-cw-and-ccw-tarot-1655

[7] Piezo element PPA-1021 Web site: www.mouser.com/datasheet/2/606/ppa-piezo-product-datasheet-844547.pdf

[8] SolidWorks Web site: www.solidsolutions.co.uk

[9] Creo pro engineer Web site: www.ptc.com/en/products/creo/pro-engineer

[10] Static thrust calculation Web site: www.quadcopterproject.wordpress.com/static-thrust-calculation/

[11] Online thrust calculator Web site: www.poweredparagliders.com.au/Calculators/Static_Thrust_Calculator.htm

[12] Hengli KV 370 motor Web site: www.rchobby-avenues.co.uk/hengli-w4830-kv370-brushless-outrunner-disk-motor-x2-hengli-w4830

[13] Electronic Speed Controller (ESC) Web site: www.dji.com/uk/takyon-z318-and-z420

[14] OneShot125 PWM protocol Web site: www.ardupilot.org/plane/docs/common-brushless-escs.html

BIOGRAPHY

Leonid Shpanin *received the M.Sc. degree in radio engineering from Azerbaijan Technical University, Baku, Azerbaijan, and the Ph.D. degree in electrical and electronic engineering from the University of Liverpool, U.K. He is a Senior Lecturer in Electronic Engineering and M.Sc. course leader in automation, control and robotics, Department of Engineering and Mathematics, Sheffield Hallam University, U.K. He is a guest member of an international study Low-Voltage group on switchgear arcs, which is a part of the Current Zero Club, Senior member of IEEE, USA and a fellow of the higher education academy, UK.*

Misko Abramiuk *received his B.Sc. in Physics at Sheffiled Univesity, U.K. and M.Sc. in Electronic engineering at at Nottingham University, U.K. He is currently a technical manager at Sheffiled Hallam University, U.K. During his career at the University which spans several decades he has held several technical support roles within its technical structures in the areas of Physics, Sport technology, Electronic engineering and Instrumentation.*

Matthew Goodwin *has over 20 years' experience as an engineer after completing his toolmaking apprenticeship. Since 2013, he has been with Sheffield Hallam University, U.K. holding a role as technical specialist in the precision engineering department. This covers a wide range of engineering tasks from conventional machining to modern 5 axis Cad Cam work. One of the roles he is particularly proud of is working alongside formula student to design and build a race car. They have regularly placed in the top 25 teams at the event in Silverstone.*

Kannan Bernard Parameswaran Vetteel *received the M.Sc. degree in automation, control and robotics from Sheffield Hallam University, UK. He is currently studing the Master degree in Business Administration at the Universiity of Sunderland, UK to enhance his education linking an engineering foundation with management skills, with innovative thinking in the professional world.*

Aasish Karuva Chalil *received the M.Sc. degree in automation, control and robotics from Sheffield Hallam University, UK. He is with Eternal Robotics PVT Ltd, India, employed as the engineer in AI and robotics working on optimizing computer vision solutions for memory-constrained devices. He has successfully deployed scalable computer vision solutions for major clients at Eternal Robotics, where he focuses on edge device deployment and client interactions. His expertise and innovation continue to drive advancements in the field.*

Nneka Osuchukwu *received her BEng & M.Sc. in Aerospace Engineering from Coventry University, U.K., and her M.Sc. in Engineering Project Management from the same institute. She currently holds the role of Scrum Master & Assistant Project Manager, working on strategic engineering projects in the rail industry. Since 2018, her career has focused on roles within the Compressed Air Industry, as well as integral positions on IT & Rail Engineering projects.*

Nicholas Pickett *obtained his M.Phil. in computer-aided design and manufacture from Cranfield University. He is currently a Principal Lecturer in the Department of Engineering and Maths at Sheffield Hallam University, U.K. He was the subject lead for mechanical engineering but has changed his role to lead the department's knowledge exchange and knowledge transfer partnership activities. He has spent more than 25 years working with industry to provide innovative solutions to a range of engineering problems. He is also a keen advocate for Science, Technology, Engineering and Maths (STEM), and regularly supports local charities and initiatives to encourage young people to consider a career in STEM.*